Neuron

Article

A neural substrate for short-term taste memories

Graphical abstract

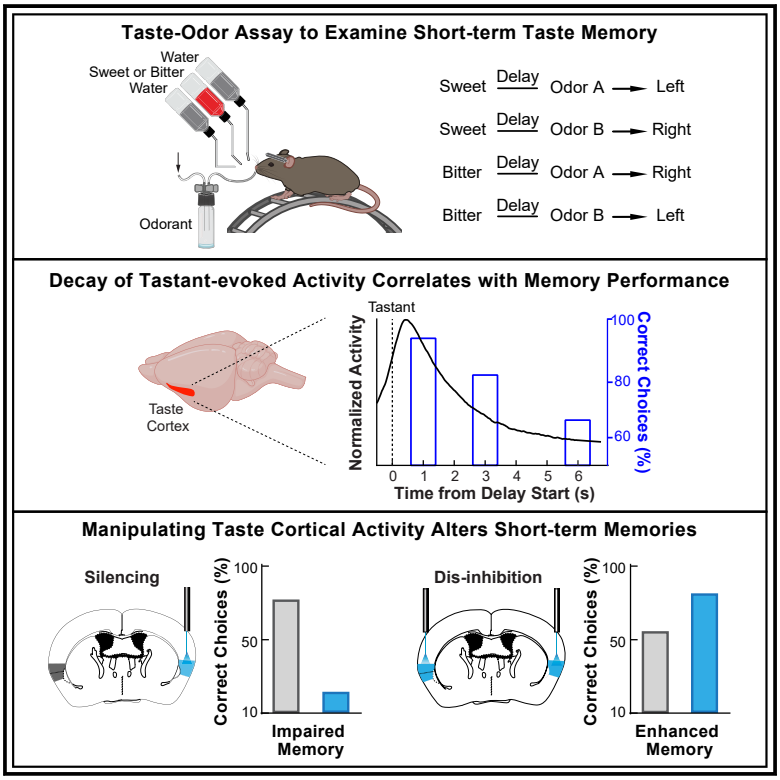

Highlights

- Taste cortex exhibits persistent activity that outlasts the taste stimulus
- The decay of persistent activity represents the decay of short-term memory
- Early termination of the persistent activity abolishes the short-term memory
- Extending the decay of persistent activity extends the taste memory

Authors

Zhang Juen, Miguel Villavicencio, Charles S. Zuker

Correspondence

jz2956@columbia.edu (Z.J.), cz2195@columbia.edu (C.S.Z.)

In brief

Sensory cortices have long been proposed to play a role in working memory. Juen et al. demonstrate that persistent activity in gustatory cortex functions as a memory trace of a recent taste experience. They show that by manipulating the duration of persistent activity, they abolish or enhance short-term taste memories.

Juen et al., 2024, Neuron *112*, 277–287
January 17, 2024
https://doi.org/10.1016/j.neuron.2023.10.009

CellPress

Neuron

CellPress
OPEN ACCESS

Article

A neural substrate for short-term taste memories

Zhang Juen,[1,2,3,5,*] Miguel Villavicencio,[1,2,3] and Charles S. Zuker[1,2,3,4,*]
[1]Howard Hughes Medical Institute
[2]Department of Biochemistry and Molecular Biophysics, Columbia University, New York, NY 10032, USA
[3]Zuckerman Mind Brain and Behavior Institute, Columbia University, New York, NY 10032, USA
[4]Department of Neuroscience, Vagelos College of Physicians and Surgeons, Columbia University, New York, NY 10032, USA
[5]Lead contact
*Correspondence: jz2956@columbia.edu (Z.J.), cz2195@columbia.edu (C.S.Z.)
https://doi.org/10.1016/j.neuron.2023.10.009

SUMMARY

Real-time decisions on what foods to select for consumption, particularly in the wild, require a sensitive sense of taste and an effective system to maintain short-term taste memories, also defined as working memory in the scale of seconds. Here, we used a behavioral memory assay, combined with recordings of neural activity, to identify the brain substrate for short-term taste memories. We demonstrate that persistent activity in taste cortex functions as an essential memory trace of a recent taste experience. Next, we manipulated the decay of this persistent activity and showed that early termination of the memory trace abolished the memory. Notably, extending the memory trace by transiently disinhibiting taste cortical activity dramatically extended the retention of a short-term taste memory. Together, our results uncover taste cortex as a neural substrate for working memory and substantiate the role of sensory cortex in memory-guided actions while imposing meaning to a sensory stimulus.

INTRODUCTION

The taste system is responsible for detecting and responding to the five basic taste qualities: sweet, umami, bitter, sour, and salty.[1,2] Sweet and umami taste-receptor cells (TRCs) promote the ingestion of energy-rich and protein-rich food sources,[2,3] respectively, whereas bitter and sour TRCs ensure aversion to toxic and spoiled (acid/fermented) foods.[2,3] Salt-sensing TRCs detect and help maintain sodium balance.[2–4]

Over the past several years, we have identified the TRCs and receptors mediating all five taste qualities (see for example Zhao et al.,[5] Mueller et al.,[6] Chandrashekar et al.,[7] and Zhang et al.[8]), and showed that taste signals from TRCs are transferred via labeled lines to matching taste neurons,[8,9] such that sweet TRCs connect to sweet ganglion neurons,[10] and they, in turn, enter the brain to connect with matching brainstem neurons tuned to sweet taste (i.e., in the rostral nucleus of the solitary tract [rNST][11]); similar logic applies to labeled lines connecting bitter TRCs to bitter neurons, sour to sour, and so forth.[8,10,11] From the rNST, taste signals travel to the parabrachial nucleus, then the ventral posteromedial nucleus of the thalamus, and finally to the gustatory cortex in the insula, where information about different tastes is represented by different cortical neurons.[2,12–15] Gustatory cortex, in turn, communicates with other brain areas, including those involved in valence, feeding, emotions, multisensory integration, and the internal state, to drive taste-evoked behaviors.[16–19] Importantly, the hardwired organization of the taste system does not mean that taste is not subjected to modulation or plasticity,[11] it means that these innate behaviors are predetermined, independent of learning or experience.

As animals forage for food, they must be capable of holding a memory trace of their recent taste experiences to compare and contrast the potential food choices and make the appropriate decisions.[20,21] A number of studies have suggested that the storage of short-term memories may involve the same cortical areas that encode the stimulus features.[22–30] In this regard, persistent activity has been observed in the somatosensory cortex of monkeys[23] and in the early visual cortex,[22,24] auditory cortex,[27,30] and piriform cortex[29] of animals performing delayed-response tasks. Here, we combined behavior, physiology, and activity recordings to examine stimulus-evoked activity in taste cortex and then manipulated the persistent activity to directly demonstrate that it represents a memory trace of the animal's recent taste experience.

RESULTS

A short-term taste memory assay

We implemented a behavioral assay in mice, where animals placed on a running wheel learned to lick a taste cue from a sample spout and, after a variable delay period, to report the identity of the tastant by going to the appropriate reward port (Figure 1A)[31–34]; correct responses were rewarded with water (mice were thirsty and thus motivated to perform this task).

In our first iteration, animals were provided with random presentations of a single drop of a bitter (1 mM quinine) or a sweet

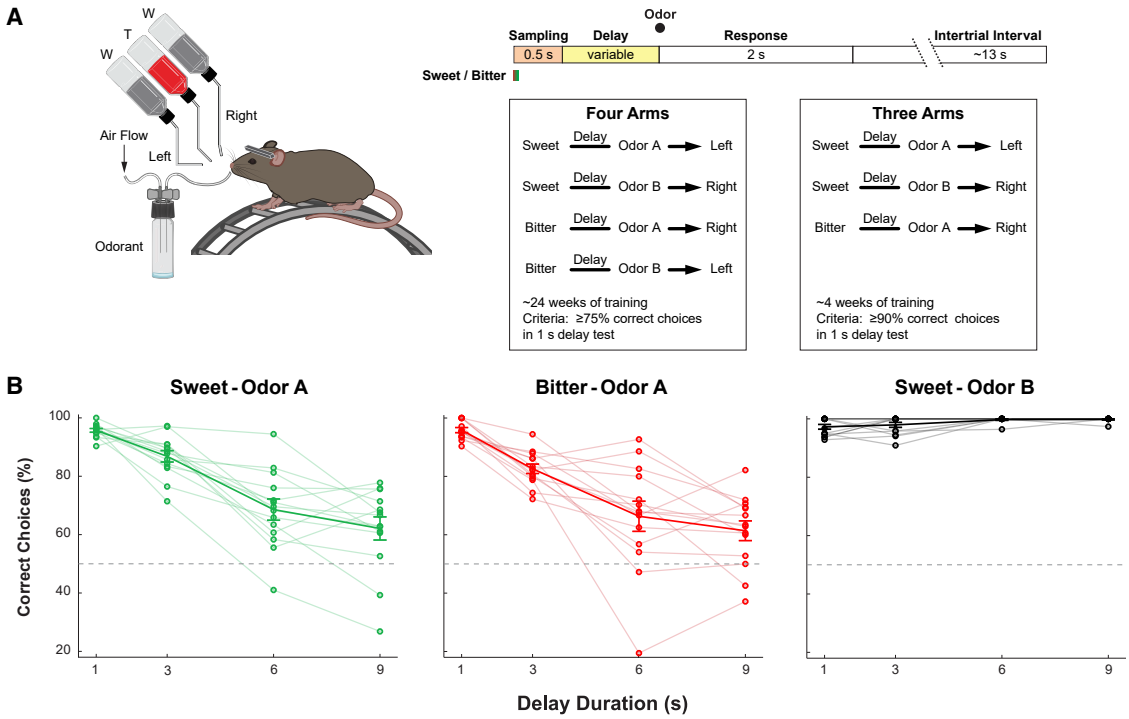

Figure 1. A short-term taste memory assay

(A) The cartoon illustrates the behavioral arena and the protocol used to examine short-term taste memories. Head-restrained mice, placed on a running wheel, were given random presentations of bitter (1 mM quinine) or sweet stimulus (5 mM AceK) from a sampling spout (middle bottle, labeled T). After a variable delay period of 1–9 s, an odor cue was presented to signal the end of delay and mark the response window (2 s). The animals were trained to report the identity of the taste stimulus by going to the left or right spout for a water reward (labeled W). Correct responses required the mice to be capable of holding the memory of the taste stimuli during the variable delay and to properly match them to the odor cue. Each session had 90–130 trials. Odor A, n-amyl acetate; odor B, benzaldehyde (see text for details). The two boxes detail the taste-odor combinations used in the four- and three-arm behavioral paradigms (see STAR Methods); also shown are the corresponding differences in training time and performance (Figure S1).

(B) Short-term taste memory performance with a 1-, 3-, 6-, and 9-s delay period in the three-arm paradigm. The graphs show the correct choices (%) for each delay. Note that the memory of the sweet odor A and bitter odor A combinations decays over time. Tastants were randomly presented in each session. Light and bold traces represent the individual and average correct choices, respectively; values are mean ± SEM; n = 14 mice. Please note that of the 14 animals tested, 8 were trained to go to the right after bitter odor A and 6 were trained to go to the left after bitter odor A, such that any potential "sideness effects" are counterbalanced.

(5 mM acesulfame K [AceK]) stimulus from the center spout and allowed to drink it for 0.5 s (total volume ~ 1 μL). Importantly, mice were trained to hold the memory of the tastant until an odor cue was presented at the end of a variable delay period (Figure 1A, see four-arms diagram); this behavioral paradigm had all possible combinations (sweet odor A, sweet odor B, bitter odor A, and bitter odor B). However, it required over 20 weeks of continuous training per animal (see STAR Methods; Figure S1). Thus, we simplified the assay to three arms (Figure 1A, three-arms diagram). Under these simpler conditions, we still greatly minimized premature licking from the water reward ports during the delay period (Figures S2 and S3), and critically, the animals also needed to hold the memory of the test stimuli during the delay period.

Mice were trained for 30–60 sessions (2 sessions/day for 3–4 weeks), each consisting of 90–130 trials. When the mice were presented with a bitter stimulus followed by odor A (n-amyl acetate) at the end of the delay, they had to choose the right port for a water reward. However, if presented with a sweet stimulus followed by the same odor A, animals had to choose the left port for the water reward. A sweet stimulus followed by odor B (benzaldehyde) required the animals to choose the right port for a water reward (see Figure 1A, three-arms diagram). At the end of the training period (see STAR Methods), mice were able to report the identity of the taste stimulus with over 90% accuracy when using a 1-s delay (Figure 1B). Because short-term memories are expected to decay as a function of time,[24,35] we then tested responses following a delay period of 3, 6, or 9 s. For the sweet odor A and bitter odor A tasks, the behavioral performance deteriorated as the duration of the delay was increased (Figure 1B, left and middle), consistent with the decay of a short-term memory trace. In the sweet odor B trials, animals were able to respond correctly, almost independently of delay time; this would be expected because recognition of the odor cue alone (odor B) is sufficient to enable the correct response (see Figure 1B, right).

Activity in gustatory cortex

Previously, we showed that gustatory cortex is essential for imposing identity to a taste stimulus (i.e., is it sweet or

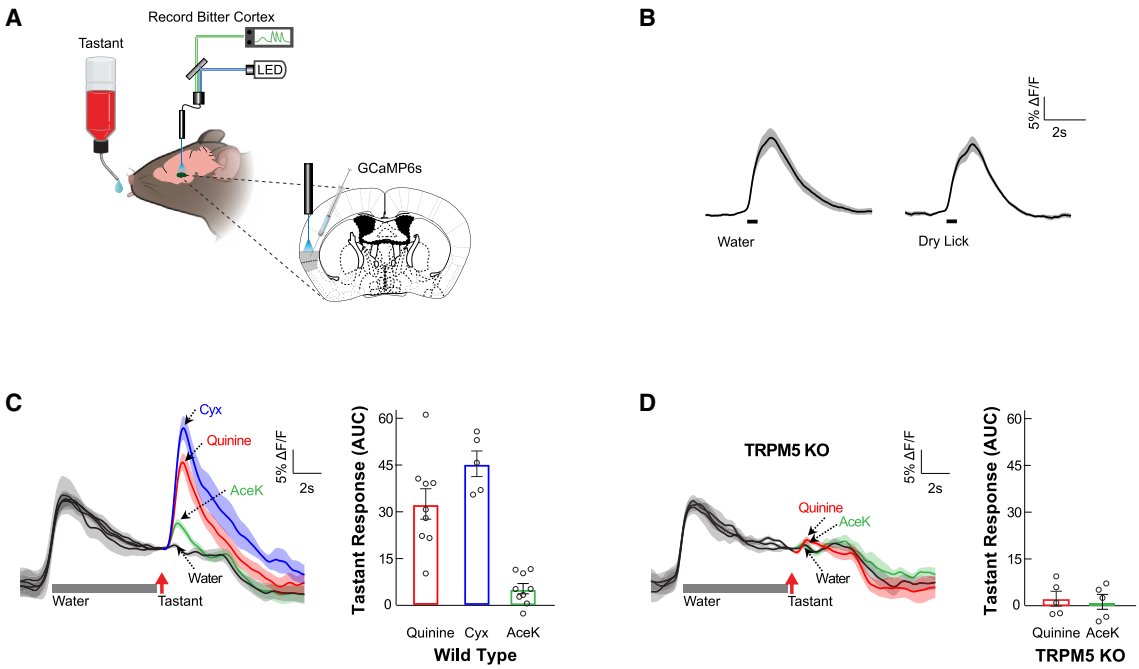

Figure 2. Measuring cortical responses to taste stimuli

(A) Schematic of fiber photometry recordings of taste-evoked activity in the GCbt. AAV-Syn-Flex-GCaMP6s and AAV-CaMKII-Cre viruses (1:1 mixture; see STAR Methods) were stereotaxically targeted to GCbt (bregma −0.35 mm) unilaterally, and a recording optical fiber was positioned above the injected site.

(B) Traces show GCaMP6s responses to water stimulation (~5 μL, 0.5 s) or to dry licks (0.5 s, see STAR Methods). Solid black lines show the average responses ± SEM (gray); n = 8 animals. Note the strong responses to water and even dry licking; these are not taste-evoked responses.

(C) GCbt neurons respond preferentially to bitter stimuli. To distinguish water licking and orofacial activity signals from tastant-evoked responses, the animals were trained to drink water for 8 s (~20 μL, gray bar) prior to delivery of the taste stimuli (1 μL, red arrow). Left: bitter stimuli evoke large responses, time locked to stimulus delivery (4 mM quinine, red trace, and 0.05 mM Cyx, blue trace). In contrast, GCbt is poorly activated by a strong sweet stimulus (20 mM AceK, green trace). Right, quantification of fiber photometry responses (Area under the curve [AUC] for the first 3 s). Values are mean ± SEM; quinine and AceK, n = 9 animals; Cyx, n = 5 animals. Individual traces are shown in Figure S4.

(D) The tastant-evoked responses depend on the activation of taste-receptor cells (TRCs) as they are missing in knockout animals unable to activate sweet and bitter TRCs. Values are mean ± SEM; n = 5 animals. Note that responses to water are unaffected.

bitter?).[12,13] We hypothesized that the sweet and bitter cortex may function as key substrates for retaining short-term taste memories. We reasoned that a short bitter stimulus would trigger strong short-term memories and therefore focused our work on bitter-evoked responses.

In the taste cortex (insula), bitter-responding neurons are greatly enriched in the posterior insula (hereafter referred to as "Gustatory Cortex-bitter" and abbreviated GCbt; bregma −0.15 to −0.5 mm).[12–15,18] Thus, we infected GCbt of wild-type mice with a mixture of AAV-CaMKII-Cre and AAV-Synapsin-Flex-GCaMP6s constructs,[36] so as to drive expression of the genetically encoded calcium indicator GCaMP6s in GCbt neurons, and used fiber photometry[37] to monitor tastant-evoked responses (Figures 2A and S4–S6).

Insular cortex is known to respond robustly to water and licking (Figure 2B).[38–41] In order to distinguish these orofacial signals from tastant-evoked responses, we first allowed the animals to lick water (Figures 2C and S4) or dry licking (Figure S5B) prior to tastant delivery, so as to establish a baseline (total consumption ~ 20 μL of water, or 15 dry licks), and then presented them with 1 μL of a bitter (4 mM quinine or 50 μM cycloheximide [Cyx]) or a sweet stimulus (20 mM AceK). As expected, GCbt neurons exhibited robust, time-locked responses to bitter tastants (Figures 2C, S4, and S5B). By contrast, responses to sweet tastant were very small, even when using exceedingly strong sweet stimuli (Figures 2C, S4, and S5B). To demonstrate that these tastant-evoked responses indeed originate from the selective activation of TRCs on the tongue and represent validated cortical taste responses (rather than responses to water, licking, orofacial, or other non-taste activity, see Chen et al.[41]) we repeated the fiber photometry recording experiments in animals lacking the taste signaling channel TRPM5; this ion channel is essential for bitter and sweet signaling.[42] Indeed, all responses to bitter, as well as the small responses to sweet, were abolished in the taste cortex of the TRPM5 knockout animals (Figure 2D). Not surprisingly, responses to water were unaffected (Figure S5C). These results substantiate the tastant-dependency of the responses and further illustrate the strong representation of bitter- versus sweet-responding neurons in posterior insula.[12–15]

Next, we examined the time course of the taste responses. Notably, we observed significant persistent activity during the variable delay period, long after termination of the 0.5 s bitter taste stimulus, and with a timescale that far exceeded the

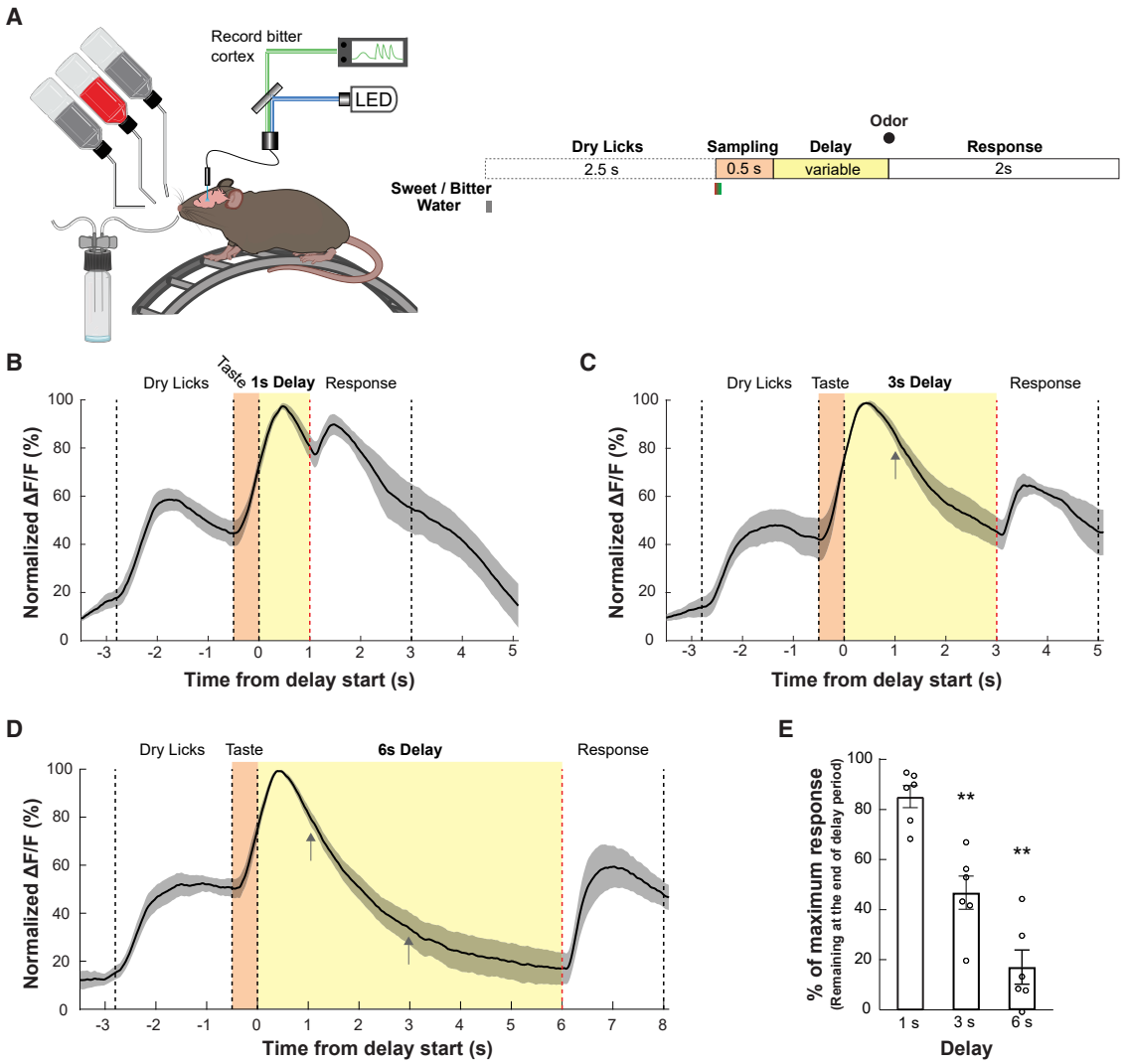

Figure 3. Persistent activity in taste cortex

(A) Schematic of photometry and short-term taste memory assay. Mice were given one drop of water (~1 μL), followed by 2.5 s of dry licks prior to the presentation of the sweet (5 mM AceK) or bitter (1 mM quinine) stimulus. The incorporation of the dry-lick window helps minimize the volume of water consumed and motivates the animals to continue performing for a water reward.

(B) Normalized average GCaMP6s responses in GCbt to the bitter odor A stimuli (black trace ± SEM), using a 1-s delay. n = 6 animals, 175 trials.

(C) Normalized average GCaMP6s responses in GCbt to the bitter odor A stimuli (black trace ± SEM), using a 3-s delay. n = 6 animals, 174 trials.

(D) Normalized average GCaMP6s responses in GCbt to the bitter odor A stimuli (black trace ± SEM), using a 6-s delay. n = 6 animals, 166 trials.

In all cases, individual responses were normalized to the maximal activity recorded for each animal (see Figures S5D–S5F for responses to sweet stimuli); graphs include correct and incorrect trials. Arrows denote the location of the 1- and 3-s delay time points. We note that the kinetics of decay of GCbt activity (i.e., persistent activity) are far longer than the spontaneous decay of GCaMP6s (see Figure S6A).[36,43–45] Also, there are no significant facial movements during the delay period on the timescale of the activity decay (Figure S7).

(E) Graph showing GCbt responses remaining at the end of delay period (red dash lines in B–D); shown is the average amplitude as a percent of the maximal response. Values are mean ± SEM; n = 6 animals; paired t test: 1 versus 3 s, ** p = 0.0023; 1 versus 6 s, p = 0.0007; 3 versus 6 s, ** p = 0.0016.

decay kinetics of the GCaMP6s reporter (Figures 3, S5D–S5F, and S6).[36,43–45] This persistent activity was detected under all variable delays and is best observed in the 6-s trials (Figure 3D).

Persistent activity is not the result of residual tastant

To confirm that the persistent activity was not a consequence of residual bitter tastant remaining on the tongue during the delay period, we performed two sets of complementary studies. First, we targeted ChR2 to the neurons in the brainstem that carry all bitter signals from the periphery into the brain,[11] and examined the responses of GCbt to a short pulse of optogenetic rather than a chemical taste stimulus (Figures 4A, S8A, and S8B; see STAR Methods for details). Our results (Figures 4B and S6D) demonstrated that a transient

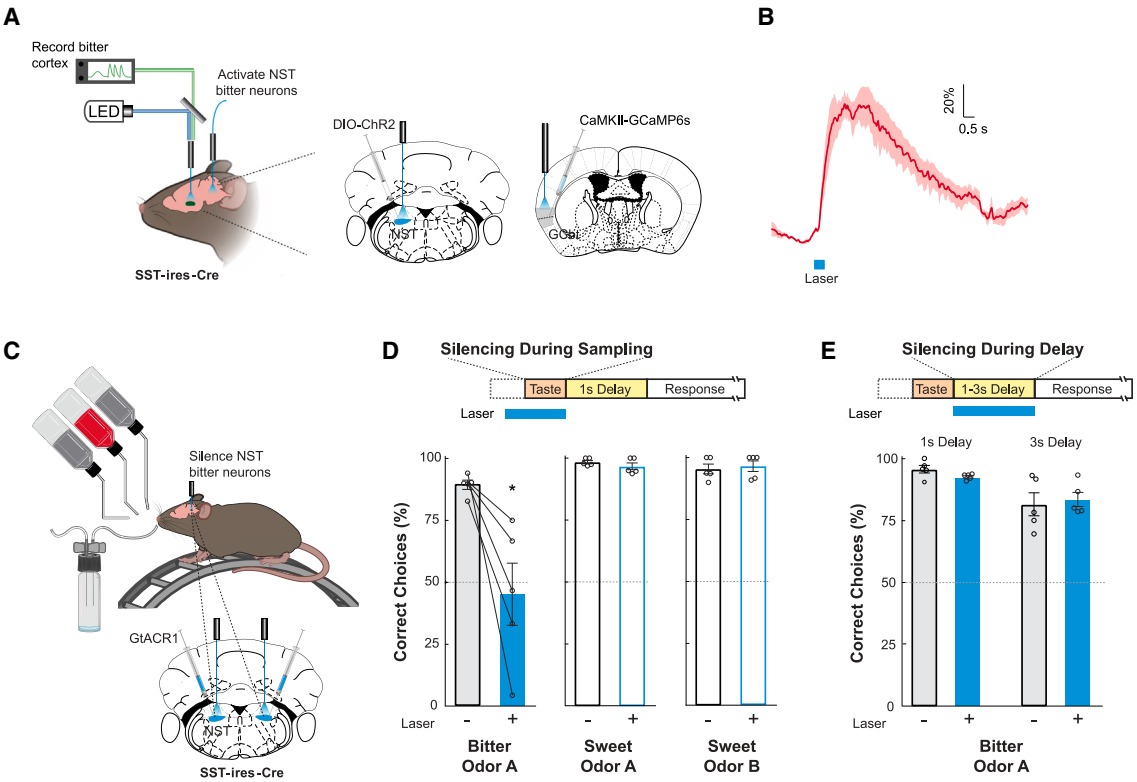

Figure 4. Persistent activity in the GCbt

(A) Schematic of photometry recordings from GCbt, and optogenetic stimulation of bitter neurons in the rostral NST (rNST). GCbt was targeted with AAV-CamKII-GCaMP6s, and the rNST of SST-ires-Cre mice was targeted ipsilaterally with an AAV-EF1α-DIO-hChR2 virus. A recording fiber for GCaMPs photometry was implanted above GCbt, and a stimulating fiber was positioned above the bitter neurons expressing ChR2 in the rNST.

(B) Responses of GCbt neurons to a 0.5 s laser pulse activating bitter neurons in rNST. The blue bar denotes the laser stimulus (see text). Average responses (±SEM) were normalized to the maximal activity recorded for each animal; n = 5 animals. For analyses of half-decay times, see Figure S6D.

(C) Silencing bitter neurons in the rNST. An AAV1-EF1α-DIO-GtACR1 virus was bilaterally injected into the rNST of SST-ires-Cre animals, and two optical stimulating fibers were implanted above each injection site.

(D) Transient optogenetic silencing of bitter neurons in the rNST during sampling of the bitter stimuli (1 mM quinine) abolished the capacity of the animal to identify the bitter tastant. In contrast, responses to sweet stimuli were unaffected. Note normal performance in laser-off trials. Values are mean ± SEM; n = 5 animals; paired t test: bitter odor A, * p = 0.0272; sweet odor A, p = 0.268; sweet odor B, p = 0.503.

(E) Silencing bitter neurons in the rNST after sampling the bitter stimuli (i.e., during the delay period) had no noticeable impact on the animals' performance. Values are mean ± SEM. Shown are results using a 1 s (paired t test, p = 0.186) or a 3 s (p = 0.649) delay; n = 5 animals. The 1- and 3-s delays were tested in different sessions.

0.5 s laser stimulus produces time-locked GCbt activation with slow-decaying, persistent activity, as was observed with chemical stimulation of the tongue (Figures 2C and 3B–3E). Second, we reasoned that if we could prevent any signals from the tongue from reaching the cortex during the delay period, we would then prevent any contribution from potential residual TRC activity. Thus, we bilaterally targeted the GtACR1 inhibitory opsin[46] to the bitter neurons in the brainstem (Figures 4C and S8C), such that all incoming bitter signals from the tongue could be experimentally blocked from continuing to the cortex.[11] We then tested the behavioral performance of these animals by comparing the effect of silencing bitter brainstem neurons during sampling versus silencing after sampling the bitter stimulus. As would be predicted, silencing during tastant sampling abolished the capacity of the animals to recognize and respond to the bitter stimuli (Figure 4D). Notably, silencing after sampling, during the variable delay period, had no effect on the animals' short-term taste memory, with performance indistinguishable from the control trials (Figures 4E and S8D). Together, these results demonstrated that signaling from the tongue during the delay window is not a contributor to the animal's performance and that the tastant-evoked persistent activity in GCbt can be recapitulated even by a transient fictive (optogenetic) bitter stimuli.

Gustatory cortex holds short-term taste memories

If the persistent activity of GCbt is the neural substrate for short-term taste memories, we made three predictions: first, the time course of decay of the memory trace should correlate with the animal's short-term memory performance. Second, transient silencing of taste cortex during the variable delay should erase the memory trace. Finally, extending the decay should help preserve the short-term memory for a longer time and,

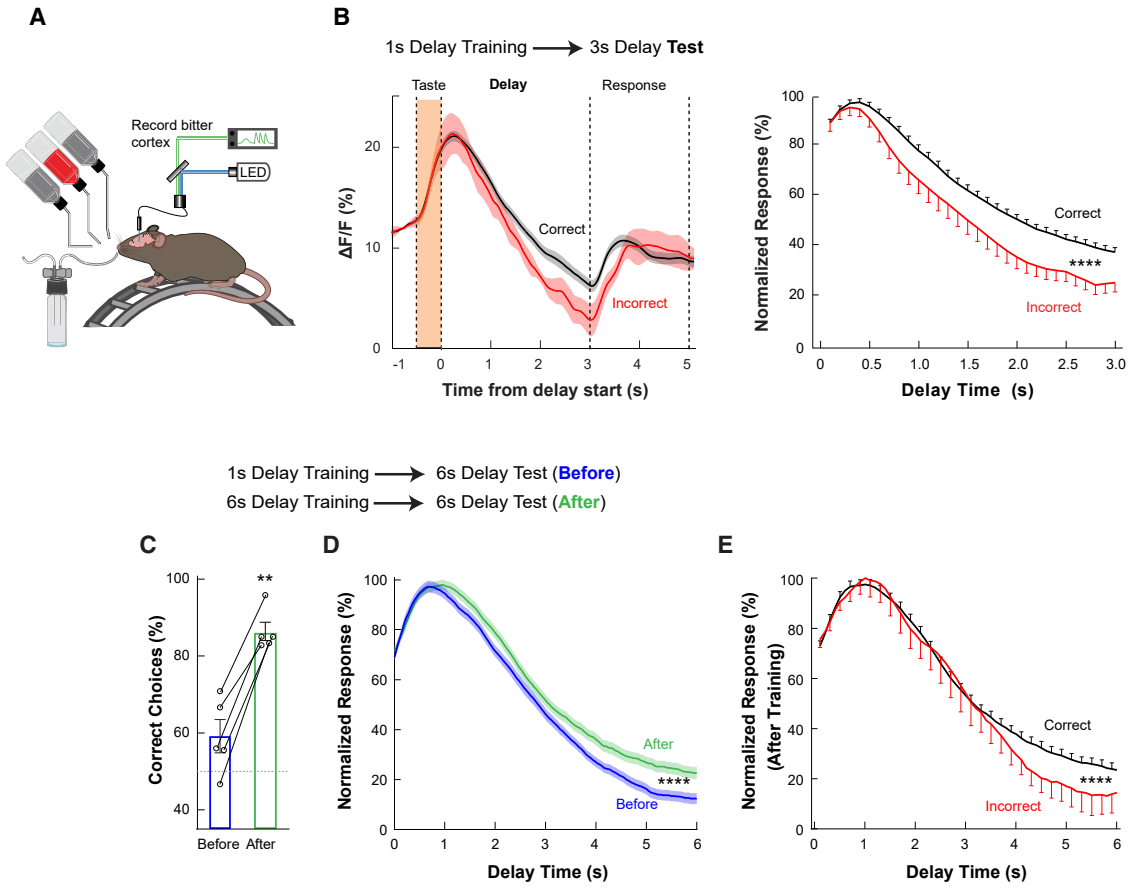

Figure 5. Decay of taste cortical activity mirrors behavioral performance

(A) Schematic of GCbt photometry recordings during the short-term taste memory tests.

(B) Shown are sample traces of activity in GCbt to the bitter odor A stimuli for one animal, from delivery of the stimuli (taste) to response. The black trace denotes average responses for trials where the mouse correctly identified the bitter stimuli after a 3-s delay period (correct). The red trace shows average responses in trials that produced incorrect responses (total for this example: 37 trials; 32 correct and 5 incorrect). The right panel shows the summary of decay traces for 6 different mice. Plotted is the normalized average GCaMP6s signals during the 3-s delay window in GCbt. Responses were normalized to the maximal activity recorded in each trial. Values are mean ± SEM; n = 6 animals; correct, 119 trials; incorrect, 33 trials; Kruskal-Wallis test: **** $p < 0.0001$. For analyses of half-decay times, see Figure S6E.

(C) When animals were trained on the short-term taste memory assay using a delay of 6 s (instead of the standard 1-s delay), their short-term memory performance improved from being correct in less than 60% of the trials to over 80% correct. Values are mean ± SEM; n = 5 animals; Mann-Whitney test: ** $p = 0.0022$. We note that approximately 30% of the animals did not meet the criteria for inclusion for testing after 6-s delay training (>70% correct responses after the 10 days of training with a 6-s delay; see STAR Methods).

(D) Shown are traces of activity in GCbt during the 6-s delay window for animals that were trained using the standard 1-s delay but tested using a 6-s delay (Before) versus animals that were trained using a 6-s delay window and tested with the same 6-s delay (After). GCaMP6s responses were normalized to the maximal activity recorded in each trial. Values are mean ± SEM; n = 5 animals; before, 132 trials; after, 146 trials; Kruskal-Wallis test: **** $p < 0.0001$. For analyses of half-decay times see Figure S6F.

(E) Shown is summary of decay traces for mice trained and tested with the 6-s delay (green trace in C). Plotted is the normalized average GCaMP6s signals during the 6-s delay window in GCbt. Responses were normalized to the maximal activity recorded in each trial. Values are mean ± SEM; n = 5 animals; red, 125 correct trials; black, 21 incorrect trials; Kruskal-Wallis test: **** $p < 0.0001$.

correspondingly, lead to an improvement in the animal's short-term memory performance.

We asked whether the time course of the decay is correlated with performance by comparing trials that produced correct responses with those that produced incorrect responses.[24] Our results revealed a difference in the time course of the memory trace, with correct trials exhibiting statistically significant prolonged GCbt activity (Figures 5A, 5B, and S6E). Next, we hypothesized that training mice using a 6-s delay (rather than the standard 1-s delay; see STAR Methods) should extend the decay time and significantly improve the animals short-memory performance in the 6-s delay tests, in essence, by having the animals learn to hold the memory of the tastant for a full 6 s before receiving a reward. Indeed, animals improved their short-term memory performance, from initially being correct in only ~60% of the trials to well over 80% correct (Figure 5C), and as predicted, they showed a correlated change in the decay of the memory

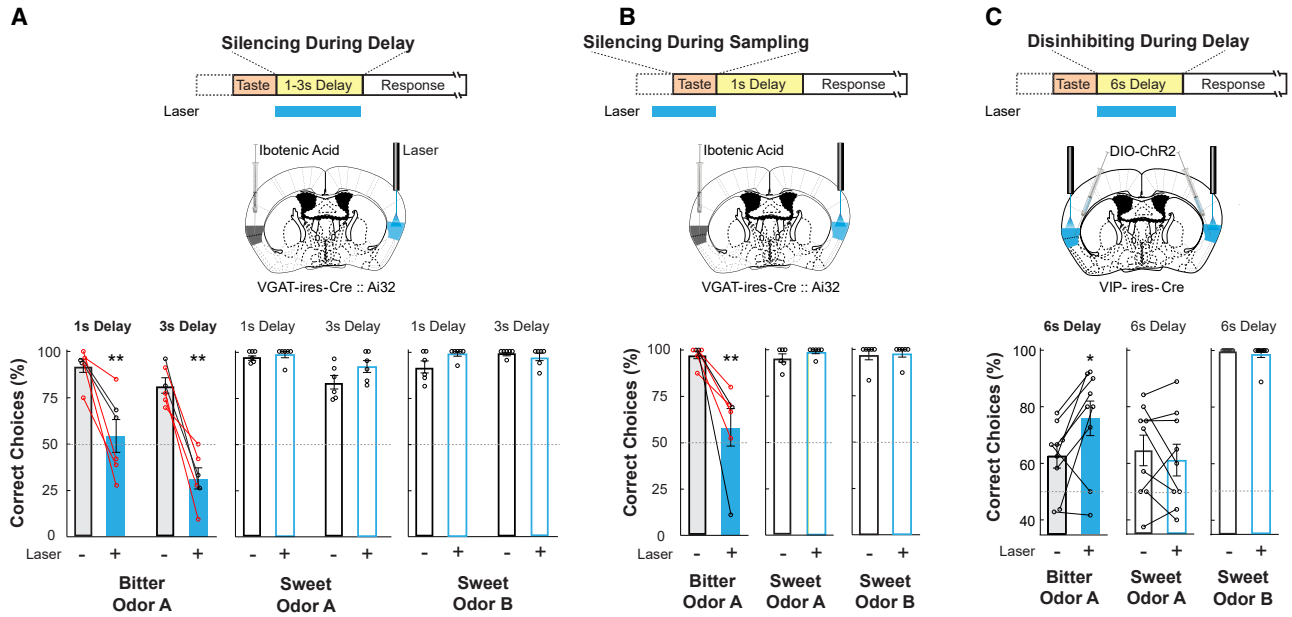

Figure 6. Short-term taste memory in gustatory cortex

(A) Silencing GCbt during the delay period abolishes short-term taste memory. Top, the diagram shows the strategy used to silence GCbt neurons. An optic fiber was unilaterally implanted above GCbt in VGAT-ires-Cre::Ai32 mice to activate GABAergic interneurons. To maximize the efficiency of silencing, we ablated the contralateral GCbt with ibotenic acid (see STAR Methods and Figures S9D–S9F). Bottom, quantification of correct choices in the short-term memory assay. The laser was on during the entire delay period; different sessions were used for 1- and 3-s delays. Values are mean ± SEM; n = 6 animals; Mann-Whitney test: bitter odor A, ** p = 0.0043 for 1-s delay, ** p = 0.0022 for 3-s delay; sweet odor A, p = 0.54 for 1-s delay, p = 0.17 for 3-s delay; sweet odor B, p = 0.11 for 1-s delay, and p = 0.45 for 3-s delay. Note selective loss of bitter, but not sweet short-term memory. Similar results were obtained with either side lesioned (right lesion, black lines; left lesion, red lines).

(B) Silencing GCbt during sampling abolished bitter taste recognition. Top, the diagram shows the strategy to silence GCbt neurons during sampling. The laser was turned on ~0.2 s before sampling and turned off at the end of the sampling window. Bottom, quantification of correct choices. Values are mean ± SEM; n = 6 animals; Mann-Whitney test: bitter odor A, ** p = 0.0022; sweet odor A, p = 0.30; sweet odor B, p = 0.99.

(C) Disinhibiting GCbt enhances short-term taste memory. Top, the diagram shows the strategy to disinhibit GCbt neurons. GCbt was bilaterally infected with AAV-EF1α-DIO-hChR2 in VIP-ires-Cre mice, and animals were trained in the memory test using a 1-s delay. Bottom, quantification of correct choices. The test delay duration was 6 s, and the laser was for 5 s of the delay period. Values are mean ± SEM; n = 9 animals; Mann-Whitney test: bitter odor A, * p = 0.047; sweet odor A, p = 0.71; and sweet odor B, p = 0.99.

trace when compared to the responses prior to 6 s training (Figures 5D, 5E, and S6F).

Our strategy to erase the memory trace was to optogenetically stimulate inhibitory interneurons[32,47] in the GCbt during the variable delay, in essence terminating the persistent activity of bitter-activated neurons. First, we used slice recordings from GCbt to demonstrate that transiently activating VGAT-expressing inhibitory interneurons effectively abolished activity in excitatory neurons (Figures S9A–S9C). Next, we generated VGAT-ires-Cre mice expressing ChR2,[48,49] implanted a stimulating fiber above GCbt (Figures S9D–S9F; see STAR Methods) and examined the animal's short-term memory performance in control trials versus trials coupled to optogenetic activation of inhibitory interneurons. Indeed, when we silenced GCbt during the variable delay, the mice were no longer capable of holding the memory of the bitter taste; the results shown in Figure 6A demonstrate that trials coupled to optogenetic activation of VGAT neurons have a dramatic loss of performance. Next, we repeated these experiments but silenced only during the last 1 s of a 3-s delay period, or only during the last 2 s of a 6-s delay period (in animals trained with 6 s). Both sets of experiments effectively abolished short-term memory (Figure S10). Together, these results further demonstrate that continuous activity is required to maintain the memory trace.

As anticipated, if VGAT neurons in GCbt were activated during the sampling of the bitter stimulus (rather than during the variable delay period), animals could no longer recognize and respond to the bitter tastant (Figure 6B). In contrast, no effect on memory performance for control sweet trials was observed (Figures 6A and 6B; see also Peng et al.[13]).

We also designed an experiment that would increase GCbt activity during the delay period. A priori, we recognized that re-activating GCbt excitatory neurons during the delay would not be suitable because it would mimic the effect of providing the animal with a new fictive bitter stimulus.[13] Recently, a number of groups have shown that activation of vasoactive intestinal polypeptide (VIP)-expressing neurons causes disinhibition of pyramidal cells by suppressing the activity of inhibitory interneurons,[33,50–52] hence changing the inhibitory-excitatory balance. To validate the approach, we prepared tissue slices for patch clamp recordings of GCbt from animals engineered to express both a ChR2 in

VIP interneurons[53] and a red-shifted ChrimsonR[54] in the thalamo-cortical taste projections (i.e., to mimic taste-evoked stimulation; Figure S11A; see STAR Methods). Our results demonstrated that activation of VIP interneurons substantially disinhibited and enhanced GCbt activity evoked by activation of the taste pathway (i.e., the thalamo-cortical taste projections) (Figures S11B–S11D). Therefore, we implemented this strategy to reversibly disinhibit cortical activity in GCbt of awake behaving animals during the variable delay period,[33] in essence extending the memory trace of bitter-evoked activity *in vivo*.

We bilaterally targeted an AAV-DIO-ChR2 to the GCbt of VIP-ires-Cre mice and waited for 2 weeks for expression in VIP interneurons. Animals were then trained and tested in the short-term taste memory assay. Remarkably, when the VIP neurons in GCbt were optogenetically activated during the delay period (6 s), immediately following presentation of bitter stimuli, there was a dramatic change in memory performance, with responses now improving from approximately 60% correct to over 75% correct in the laser-on trials (Figure 6C; compare laser-on with laser-off). As expected, the effect is specific only to bitter taste, with no impact on sweet responses. Importantly, activation of the VIP neurons in the absence of bitter stimuli does not evoke a bitter response (see Figure S12).

Taken together, these results illustrate how experimentally manipulating persistent activity in GCbt can profoundly alter the capacity of the animal to maintain the memory of a taste stimulus and substantiate taste cortex as a substrate for short-term taste memories.

DISCUSSION

Short-term taste memories operate as working memory and afford animals the critical capacity to compare and contrast potential food sources in real time. In this study, we investigated the neural basis of short-term taste memory and focused our work on bitter taste. Previously, we demonstrated that bitter and sweet are represented in taste cortex (the insula) by different neurons tuned to each taste, and showed topographic segregation between bitter and sweet neurons.[12,13,18] In addition to taste, insular cortex is activated by a variety of stimuli, including orofacial responses, licking, water, and multisensory integration.[16,19,38–41] Therefore, to extract tastant-evoked signals (versus other signals triggered by the stimulus), we implemented the use of fiber photometry combined with genetic validation to demonstrate that the cortical signals indeed originate from the activation of taste-receptor responses (Figures 2C and 2D); this fundamental genetic loss-of-function test can critically distinguish taste versus non-taste responses (a problem that often confuses the analysis of taste-evoked responses in insular cortex[41]). We also introduced a water/dry-lick window prior to tastant stimulation so as to desensitize responses to licking and focus on taste-evoked responses.

Here, we demonstrated that insular cortex functions as a neural substrate for short-term taste memories (i.e., working memory). We showed that persistent activity in gustatory cortex functions as a memory trace, providing the animal with an active repository of its recent taste experience. As would be expected, the decay of this memory trace is directly correlated to performance in a memory task. Although the work in this study focused on bitter memories, we anticipate that similar logic will apply to sweet and the other basic tastes.

We also showed that experimental manipulation of this persistent activity can predictably alter short-term memory performance. For example, by accelerating the termination of bitter-evoked persistent activity in bitter cortex, we could effectively abolish working memory of a recent bitter stimulus, with no effect on sweet taste. By contrast, by experimentally disinhibiting activity in bitter cortex (i.e., extending the decay of the memory trace), we could dramatically enhance the animal's ability to maintain and recall a bitter taste memory even after a long delay period.

Post-stimulus persistent activity has been observed in other sensory cortices, including V1 in visual cortex, piriform neurons in olfactory cortex, S1 in somatosensory cortex, and primary auditory cortex.[23,24,27,29,30] Also, sustained activity in anterior lateral motor cortex has been reported to represent motor planning.[32,55] However, a direct causal relationship between persistent activity in sensory cortices and the encoding of working memory has been elusive. The experiments described in this study substantiate primary sensory cortex as a selective neural substrate for the encoding of working memory. These results also illustrate how it is possible to manipulate cortical activity and behavioral responses for one taste (i.e., bitter) independently of others (i.e., sweet; see also Peng et al.[13]).

Recently, Vincis et al.[56] showed that insular cortex, outside of the bitter and sweet fields,[12–15,18] was activated during the performance of a sweet and bitter guided decision-making task. Notably, silencing this area had no impact on sweet or bitter tastant recognition,[56] indicating that this activity is not required to recognize sweet or bitter stimuli. Also, Chen et al.[41] used two-photon imaging to examine taste representations in this area of insular cortex and reported a sparse and distributed pattern of neuronal activity. However, a previous study using taste knockout animals[12] showed that such sparse and distributed activity was not dependent on the activation of TRCs (i.e., the same stimulus-evoked sparse activity was observed in animals that lacked functional taste receptors). It would be important to identify the nature of the stimulus that produces such sparse, distributed activity and its role in taste-receptor-dependent behaviors. By point of contrast, silencing insular cortex in the sweet or bitter fields[13,18] completely abolished the capacity of the animals to recognize sweet or bitter, respectively, and tastant-evoked neuronal activity was absent in animals lacking functional taste signaling (Figure 2) or taste receptors.[12]

The taste cortex connects to a number of cortical and subcortical brain areas (e.g., thalamus, amygdala, frontal cortex, and entorhinal cortex)[18] that have been implicated in memory and executive functions.[57–59] In the future, it will be of great interest to explore how this neural network guides food preferences, is modulated by the internal state, and orchestrates taste-evoked changes in behavior.

STAR★METHODS

Detailed methods are provided in the online version of this paper and include the following:

SUPPLEMENTAL INFORMATION

Supplemental information can be found online at https://doi.org/10.1016/j.neuron.2023.10.009.

ACKNOWLEDGMENTS

We particularly thank Martin Vignovich and members of the Zuker lab for advice and helpful suggestions. We also thank Richard Axel and Michael Shadlen for comments and suggestions. C.S.Z. is an investigator at the Howard Hughes Medical Institute. Figures were generated with the help of Biorender.com (licensed to Columbia University). This article is subject to HHMI's Open Access to Publications policy. HHMI lab heads have previously granted a nonexclusive CC BY 4.0 license to the public and a sublicensable license to HHMI in their research articles. Pursuant to those licenses, the author-accepted manuscript of this article can be made freely available under a CC BY 4.0 license immediately upon publication.

AUTHOR CONTRIBUTIONS

Z.J. performed the experiments, designed the study, analyzed data, and wrote the paper. M.V. performed behavioral and physiological experiments, designed the four-arm test, analyzed data, and wrote the paper. C.S.Z. designed the study, analyzed data, and wrote the paper.

DECLARATION OF INTERESTS

The authors declare no competing interests.

INCLUSION AND DIVERSITY

One or more of the authors of this paper self-identifies as an underrepresented ethnic minority in their field of research or within their geographical location. *We support inclusive, diverse, and equitable conduct of research.*

Received: February 20, 2023
Revised: July 18, 2023
Accepted: October 9, 2023
Published: November 8, 2023

REFERENCES

1. Scott, K. (2005). Taste recognition: food for thought. Neuron *48*, 455–464. https://doi.org/10.1016/j.neuron.2005.10.015.
2. Yarmolinsky, D.A., Zuker, C.S., and Ryba, N.J.P. (2009). Common sense about taste: from mammals to insects. Cell *139*, 234–244. https://doi.org/10.1016/j.cell.2009.10.001.
3. Lindemann, B. (1996). Taste reception. Physiol. Rev. *76*, 719–766. https://doi.org/10.1152/physrev.1996.76.3.719.
4. Bigiani, A. (2020). Salt taste, nutrition, and health. Nutrients *12*, 1537. https://doi.org/10.3390/nu12051537.
5. Zhao, G.Q., Zhang, Y., Hoon, M.A., Chandrashekar, J., Erlenbach, I., Ryba, N.J.P., and Zuker, C.S. (2003). The receptors for mammalian sweet and umami taste. Cell *115*, 255–266. https://doi.org/10.1016/S0092-8674(03)00844-4.
6. Mueller, K.L., Hoon, M.A., Erlenbach, I., Chandrashekar, J., Zuker, C.S., and Ryba, N.J.P. (2005). The receptors and coding logic for bitter taste. Nature *434*, 225–229. https://doi.org/10.1038/nature03352.
7. Chandrashekar, J., Kuhn, C., Oka, Y., Yarmolinsky, D.A., Hummler, E., Ryba, N.J.P., and Zuker, C.S. (2010). 2010-nature-The cells and peripheral representation of sodium taste in mice. Nature *464*, 297–301. https://doi.org/10.1038/nature08783.
8. Zhang, J., Jin, H., Zhang, W., Ding, C., O'Keeffe, S., Ye, M., and Zuker, C.S. (2019). Sour sensing from the tongue to the brain. Cell *179*, 392–402.e15. https://doi.org/10.1016/j.cell.2019.08.031.
9. Barretto, R.P.J., Gillis-Smith, S., Chandrashekar, J., Yarmolinsky, D.A., Schnitzer, M.J., Ryba, N.J.P., and Zuker, C.S. (2015). The neural representation of taste quality at the periphery. Nature *517*, 373–376. https://doi.org/10.1038/nature13873.
10. Lee, H., Macpherson, L.J., Parada, C.A., Zuker, C.S., and Ryba, N.J.P. (2017). Rewiring the taste system. Nature *548*, 330–333. https://doi.org/10.1038/nature23299.
11. Jin, H., Fishman, Z.H., Ye, M., Wang, L., and Zuker, C.S. (2021). Top-down control of sweet and bitter taste in the mammalian brain. Cell *184*, 257–271.e16. https://doi.org/10.1016/j.cell.2020.12.014.
12. Chen, X., Gabitto, M., Peng, Y., Ryba, N.J.P., and Zuker, C.S. (2011). A Gustotopic map of taste qualities in the mammalian brain. Science *333*, 1262–1266. https://doi.org/10.1126/science.1204076.
13. Peng, Y., Gillis-Smith, S., Jin, H., Tränkner, D., Ryba, N.J.P., and Zuker, C.S. (2015). 2015-nature-Sweet and bitter taste in the brain of awake behaving animals. Nature *527*, 512–515. https://doi.org/10.1038/nature15763.
14. Gehrlach, D.A., Dolensek, N., Klein, A.S., Roy Chowdhury, R., Matthys, A., Junghänel, M., Gaitanos, T.N., Podgornik, A., Black, T.D., Reddy Vaka, N., et al. (2019). Aversive state processing in the posterior insular cortex. Nat. Neurosci. *22*, 1424–1437. https://doi.org/10.1038/s41593-019-0469-1.
15. Dolensek, N., Gehrlach, D.A., Klein, A.S., and Gogolla, N. (2020). Facial expressions of emotion states and their neuronal correlates in mice. Science *368*, 89–94. https://doi.org/10.1126/science.aaz9468.
16. de Araujo, I.E., and Simon, S.A. (2009). The gustatory cortex and multisensory integration. Int. J. Obes. (Lond) *33*, S34–S43. https://doi.org/10.1038/ijo.2009.70.
17. Gogolla, N. (2017). The insular cortex. Curr. Biol. *27*, R580–R586. https://doi.org/10.1016/j.cub.2017.05.010.
18. Wang, L., Gillis-Smith, S., Peng, Y., Zhang, J., Chen, X., Salzman, C.D., Ryba, N.J.P., and Zuker, C.S. (2018). The coding of valence and identity in the mammalian taste system. Nature *558*, 127–131. https://doi.org/10.1038/s41586-018-0165-4.
19. Livneh, Y., and Andermann, M.L. (2021). Cellular activity in insular cortex across seconds to hours: sensations and predictions of bodily states. Neuron *109*, 3576–3593. https://doi.org/10.1016/j.neuron.2021.08.036.
20. Bermúdez-Rattoni, F. (2004). Molecular mechanisms of taste-recognition memory. Nat. Rev. Neurosci. *5*, 209–217. https://doi.org/10.1038/nrn1344.
21. Gal-Ben-Ari, S., and Rosenblum, K. (2011). Molecular mechanisms underlying memory consolidation of taste information in the cortex. Front. Behav. Neurosci. *5*, 87. https://doi.org/10.3389/fnbeh.2011.00087.
22. Fuster, J.M. (1990). Inferotemporal units in selective visual attention and short-term memory. J. Neurophysiol. *64*, 681–697. https://doi.org/10.1152/jn.1990.64.3.681.

23. Zhou, Y.D., and Fuster, J.M. (1996). Mnemonic neuronal activity in somatosensory cortex. Proc. Natl. Acad. Sci. USA *93*, 10533–10537. https://doi.org/10.1073/pnas.93.19.10533.

24. Supèr, H., Spekreijse, H., and Lamme, V.A.F. (2001). A neural correlate of working memory in the monkey primary visual cortex. Science *293*, 120–124. https://doi.org/10.1126/science.1060496.

25. Pasternak, T., and Greenlee, M.W. (2005). Working memory in primate sensory systems. Nat. Rev. Neurosci. *6*, 97–107. https://doi.org/10.1038/nrn1603.

26. Harrison, S.A., and Tong, F. (2009). Decoding reveals the contents of visual working memory in early visual areas. Nature *458*, 632–635. https://doi.org/10.1038/nature07832.

27. Huang, Y., Matysiak, A., Heil, P., König, R., and Brosch, M. (2016). Persistent neural activity in auditory cortex is related to auditory working memory in humans and nonhuman primates. eLife *5*, e15441. https://doi.org/10.7554/eLife.15441.

28. Serences, J.T. (2016). Neural mechanisms of information storage in visual short-term memory. Vision Res. *128*, 53–67. https://doi.org/10.1016/j.visres.2016.09.010.

29. Zhang, X., Yan, W., Wang, W., Fan, H., Hou, R., Chen, Y., Chen, Z., Ge, C., Duan, S., Compte, A., et al. (2019). Active information maintenance in working memory by a sensory cortex. eLife *8*, e43191. https://doi.org/10.7554/eLife.43191.

30. Yu, L., Hu, J., Shi, C., Zhou, L., Tian, M., Zhang, J., and Xu, J. (2021). The causal role of auditory cortex in auditory working memory. eLife *10*, e64457. https://doi.org/10.7554/eLife.64457.

31. Erlich, J.C., Bialek, M., and Brody, C.D. (2011). A cortical substrate for memory-guided orienting in the rat. Neuron *72*, 330–343. https://doi.org/10.1016/j.neuron.2011.07.010.

32. Guo, Z.V., Li, N., Huber, D., Ophir, E., Gutnisky, D., Ting, J.T., Feng, G., and Svoboda, K. (2014). Flow of cortical activity underlying a tactile decision in mice. Neuron *81*, 179–194. https://doi.org/10.1016/j.neuron.2013.10.020.

33. Kamigaki, T., and Dan, Y. (2017). Delay activity of specific prefrontal interneuron subtypes modulates memory-guided behavior. Nat. Neurosci. *20*, 854–863. https://doi.org/10.1038/nn.4554.

34. Wu, Z., Litwin-Kumar, A., Shamash, P., Taylor, A., Axel, R., and Shadlen, M.N. (2020). Context-dependent decision making in a premotor circuit. Neuron *106*, 316–328.e6. https://doi.org/10.1016/j.neuron.2020.01.034.

35. Jonides, J., Lewis, R.L., Nee, D.E., Lustig, C.A., Berman, M.G., and Moore, K.S. (2008). The mind and brain of short-term memory. Annu. Rev. Psychol. *59*, 193–224. https://doi.org/10.1146/annurev.psych.59.103006.093615.

36. Chen, T.W., Wardill, T.J., Sun, Y., Pulver, S.R., Renninger, S.L., Baohan, A., Schreiter, E.R., Kerr, R.A., Orger, M.B., Jayaraman, V., et al. (2013). Ultrasensitive fluorescent proteins for imaging neuronal activity. Nature *499*, 295–300. https://doi.org/10.1038/nature12354.

37. Gunaydin, L.A., Grosenick, L., Finkelstein, J.C., Kauvar, I.V., Fenno, L.E., Adhikari, A., Lammel, S., Mirzabekov, J.J., Airan, R.D., Zalocusky, K.A., et al. (2014). Natural neural projection dynamics underlying social behavior. Cell *157*, 1535–1551. https://doi.org/10.1016/j.cell.2014.05.017.

38. Stapleton, J.R., Lavine, M.L., Wolpert, R.L., Nicolelis, M.A., and Simon, S.A. (2006). Rapid taste responses in the gustatory cortex during licking. J. Neurosci. *26*, 4126–4138. https://doi.org/10.1523/JNEUROSCI.0092-06.2006.

39. Livneh, Y., Ramesh, R.N., Burgess, C.R., Levandowski, K.M., Madara, J.C., Fenselau, H., Goldey, G.J., Diaz, V.E., Jikomes, N., Resch, J.M., et al. (2017). 2017-Nature-Homeostatic circuits selectively gate food cue responses in insular cortex. Nature *546*, 611–616. https://doi.org/10.1038/nature22375.

40. Livneh, Y., Sugden, A.U., Madara, J.C., Essner, R.A., Flores, V.I., Sugden, L.A., Resch, J.M., Lowell, B.B., and Andermann, M.L. (2020). Estimation of current and future physiological states in insular cortex. Neuron *105*, 1094–1111.e10. https://doi.org/10.1016/j.neuron.2019.12.027.

41. Chen, K., Kogan, J.F., and Fontanini, A. (2021). Spatially distributed representation of taste quality in the gustatory insular cortex of behaving mice. Curr. Biol. *31*, 247–256.e4. https://doi.org/10.1016/j.cub.2020.10.014.

42. Zhang, Y., Hoon, M.A., Chandrashekar, J., Mueller, K.L., Cook, B., Wu, D., Zuker, C.S., and Ryba, N.J.P. (2003). Coding of sweet, bitter, and umami tastes: different receptor cells sharing similar signaling pathways. Cell *112*, 293–301. https://doi.org/10.1016/S0092-8674(03)00071-0.

43. Daie, K., Svoboda, K., and Druckmann, S. (2021). Targeted photostimulation uncovers circuit motifs supporting short-term memory. Nat. Neurosci. *24*, 259–265. https://doi.org/10.1038/s41593-020-00776-3.

44. Dana, H., Sun, Y., Mohar, B., Hulse, B.K., Kerlin, A.M., Hasseman, J.P., Tsegaye, G., Tsang, A., Wong, A., Patel, R., et al. (2019). High-performance calcium sensors for imaging activity in neuronal populations and microcompartments. Nat. Methods *16*, 649–657. https://doi.org/10.1038/s41592-019-0435-6.

45. Huang, L., Ledochowitsch, P., Knoblich, U., Lecoq, J., Murphy, G.J., Reid, R.C., de Vries, S.E., Koch, C., Zeng, H., Buice, M.A., et al. (2021). Relationship between simultaneously recorded spiking activity and fluorescence signal in GCaMP6 transgenic mice. eLife *10*, e51675. https://doi.org/10.7554/eLife.51675.

46. Govorunova, E.G., Sineshchekov, O.A., Janz, R., Liu, X., and Spudich, J.L. (2015). NEUROSCIENCE. Natural light-gated anion channels: a family of microbial rhodopsins for advanced optogenetics. Science *349*, 647–650. https://doi.org/10.1126/science.aaa7484.

47. Reinhold, K., Lien, A.D., and Scanziani, M. (2015). Distinct recurrent versus afferent dynamics in cortical visual processing. Nat. Neurosci. *18*, 1789–1797. https://doi.org/10.1038/nn.4153.

48. Madisen, L., Mao, T., Koch, H., Zhuo, J.M., Berenyi, A., Fujisawa, S., Hsu, Y.W., Garcia, A.J., Gu, X., Zanella, S., et al. (2012). A toolbox of Cre-dependent optogenetic transgenic mice for light-induced activation and silencing. Nat. Neurosci. *15*, 793–802. https://doi.org/10.1038/nn.3078.

49. Vong, L., Ye, C., Yang, Z., Choi, B., Chua, S., and Lowell, B.B. (2011). Leptin action on GABAergic neurons prevents obesity and reduces inhibitory tone to POMC neurons. Neuron *71*, 142–154. https://doi.org/10.1016/j.neuron.2011.05.028.

50. Lee, S., Kruglikov, I., Huang, Z.J., Fishell, G., and Rudy, B. (2013). A disinhibitory circuit mediates motor integration in the somatosensory cortex. Nat. Neurosci. *16*, 1662–1670. https://doi.org/10.1038/nn.3544.

51. Pfeffer, C.K., Xue, M., He, M., Huang, Z.J., and Scanziani, M. (2013). Inhibition of inhibition in visual cortex: the logic of connections between molecularly distinct interneurons. Nat. Neurosci. *16*, 1068–1076. https://doi.org/10.1038/nn.3446.

52. Pi, H.J., Hangya, B., Kvitsiani, D., Sanders, J.I., Huang, Z.J., and Kepecs, A. (2013). Cortical interneurons that specialize in disinhibitory control. Nature *503*, 521–524. https://doi.org/10.1038/nature12676.

53. Taniguchi, H., He, M., Wu, P., Kim, S., Paik, R., Sugino, K., Kvitsiani, D., Fu, Y., Lu, J., Lin, Y., et al. (2011). A resource of Cre driver lines for genetic targeting of GABAergic neurons in cerebral cortex. Neuron *71*, 995–1013. https://doi.org/10.1016/j.neuron.2011.07.026.

54. Klapoetke, N.C., Murata, Y., Kim, S.S., Pulver, S.R., Birdsey-Benson, A., Cho, Y.K., Morimoto, T.K., Chuong, A.S., Carpenter, E.J., Tian, Z., et al. (2014). Independent optical excitation of distinct neural populations. Nat. Methods *11*, 338–346. https://doi.org/10.1038/nmeth.2836.

55. Guo, Z.V., Inagaki, H.K., Daie, K., Druckmann, S., Gerfen, C.R., and Svoboda, K. (2017). Maintenance of persistent activity in a frontal thalamocortical loop. Nature *545*, 181–186. https://doi.org/10.1038/nature22324.

56. Vincis, R., Chen, K., Czarnecki, L., Chen, J., and Fontanini, A. (2020). Dynamic representation of taste-related decisions in the gustatory insular cortex of mice. Curr. Biol. *30*, 1834–1844.e5. https://doi.org/10.1016/j.cub.2020.03.012.

57. Panichello, M.F., and Buschman, T.J. (2021). Shared mechanisms underlie the control of working memory and attention. Nature *592*, 601–605. https://doi.org/10.1038/s41586-021-03390-w.

58. Bolkan, S.S., Stujenske, J.M., Parnaudeau, S., Spellman, T.J., Rauffenbart, C., Abbas, A.I., Harris, A.Z., Gordon, J.A., and Kellendonk, C. (2017). Neurosci-thalamic projections sustain prefrontal activity during working memory maintenance. Nat. Neurosci. *20*, 987–996. https://doi.org/10.1038/nn.4568.

59. Josselyn, S.A., and Tonegawa, S. (2020). Memory engrams: recalling the past and imagining the future. Science *367*, eaaw4325. https://doi.org/10.1126/science.aaw4325.

60. Mathis, A., Mamidanna, P., Cury, K.M., Abe, T., Murthy, V.N., Mathis, M.W., and Bethge, M. (2018). DeepLabCut: markerless pose estimation of user-defined body parts with deep learning. Nat. Neurosci. *21*, 1281–1289. https://doi.org/10.1038/s41593-018-0209-y.

STAR★METHODS

KEY RESOURCES TABLE

REAGENT or RESOURCE	SOURCE	IDENTIFIER
Bacterial and virus strains		
pENN-AAV-CamKII-Cre-SV40	a gift from James M. Wilson	Addgene AAV1; 105558-AAV1
pAAV-Syn-Flex-GCaMP6s-WPRE-SV40	a gift from Douglas Kim & GENIE Project	Addgene AAV1; 100845-AAV1
AAV-CamKII-GCaMP6s-WPRE-SV40	gift from James M. Wilson	Addgene AAV9; 107790-AAV9
pAAV-EF1a-double floxed-hChR2(H134R)-EYFP-WPRE-HGHpA	a gift from Karl Deisseroth	Addgene AAV1; 20298-AAV1
AAV1-EF1α-DIO-GtACR1-P2A-GFP	Janelia	N/A
AAV2/9-CaMKII-ChrimsonR-tdtomato	Janelia	N/A
Chemicals, peptides, and recombinant proteins		
Acesulfame K	Sigma-Aldrich	04054
Actidione (Cycloheximide)	Sigma-Aldrich	01810
Quinine monohydrochloride dihydrate	Sigma-Aldrich	145920
Ibotenic acid	Santa Cruz Biotechnology	sc-200449, CAS 2552-55-8
N-Amyl acetate	Sigma-Aldrich	W504009
Benzaldehyde	Sigma-Aldrich	W212717
Experimental models: Organisms/strains		
C57BL/6J	The Jackson Laboratory	000664
SST-IRES-Cre	The Jackson Laboratory	013044
TrpM5 -/-	Zhang et al.[42]	N/A
VGAT-IRES-Cre	The Jackson Laboratory	028862
Ai32	The Jackson Laboratory	024109
VIP-IRES-Cre	The Jackson Laboratory	010908
Software and algorithms		
Arduino	Arduino	https://www.arduino.cc/
MATLAB	MathWorks	https://www.mathworks.com/
DeepLabCut	Mathis et al.[60]	https://github.com/DeepLabCut

RESOURCE AVAILABILITY

Lead contact

Further information and requests for resources and reagents should be directed to Zhang Juen (jz2956@columbia.edu).

Materials availability

This study did not generate new unique reagents.

Data and code availability

The data and custom code that support the findings from this study are available from the lead contact upon request.

EXPERIMENTAL MODEL AND STUDY PARTICIPANT DETAILS

Animals

All procedures were performed in accordance with the U.S. National Institutes of Health (NIH) guidelines for the care and use of laboratory animals, and were approved by the Columbia University Institutional Animal Care and Use Committee. Mice at least 8 weeks of age were used in the study. These mouse strains used were purchased from the Jackson Laboratory: C56BL/6J (000664); SST-IRES-Cre (013044)[53]; VGAT-IRES-Cre (028862)[49]; Ai32 (024109)[48]; VIP-IRES-Cre(010908).[53] TRPM5 knockout mice were generated in the Zuker lab.[42]

METHOD DETAILS

Viral constructs

The following AAVs were purchased from Addgene: pAAV-Syn-Flex-GCaMP6s-WPRE-SV40 (AAV-Flex-GCaMP6s); pENN-AAV-CamKII-Cre-SV40 (AAV-CaMKII-Cre); AAV-CamKII-GCaMP6s-WPRE-SV40 (AAV-CaMKII-GCaMP6s); pAAV-EF1a-double floxed-hChR2(H134R)-EYFP-WPRE-HGHpA (AAV-DIO-ChR2). The following viruses were obtained from HHMI/Janelia Vector Core: AAV1-EF1α-DIO-GtACR1-P2A-GFP (AAV-DIO-GtACR1); AAV2/9-CaMKII-ChrimsonR-tdtomato (AAV-CaMKII- ChrimsonR).

Stereotaxic surgery

All the stereotaxic surgery procedures were carried out using aseptic technique. Mice were anesthetized with a mixture of ketamine hydrochloride (Covetrus, 1169-0703-1, 0.1mg/g, intraperitoneally) and xylazine (Covetrus, 11695-4024-1, 0.01 mg/g, intraperitoneally). Animals were then placed onto a stereotaxic frame with a closed-loop heating system to help maintain body temperature. The skin was incised at the midline to expose the skull, and a small craniotomy was made at the site above regions of interest. The viral constructs or chemicals were loaded into a pulled glass capillary and injected using a nanoliter system at 40 nl/min.

The GCbt coordinates (Paxinos stereotaxic coordinates) used for injections are relative to the bregma: anterior to posterior (AP) -0.35 mm, medial to lateral (ML) 4.1mm, dorsal to ventral (DV) 2.7 mm. Injection volumes were: 120 nl 1:1 mixture of AAV-Flex-GCaMP6s and AAV-CamKII-Cre, or 120 nl of AAV-DIO-ChR2, or 120 nl AAV- CamKII-GCaMP6s, or 100 nl 10mg/ml ibotenic acid in saline. Optic fiber implantation used the same AP and ML coordinates, and DV 2.55 mm for photometry fibers or DV 2.4 mm for optogenetic stimulating fibers.

The coordinates for rNST were as described previously.[11] Fibers were tapered by immersing into hydrofluoric acid (45%, Sigma, 339261) for 50 to 60 min, and the polymer cladding was removed by transient flame burning.

After surgery, all animals were returned to the home-cage and allowed to recover for at least one week prior to any tests.

Short-term taste memory assay

All memory assays were performed on head-restrained mice running on a running wheel (Figure 1A), and placed inside a sound attenuating cubicle (Med Associates). Three retractable spouts were placed in front of the animal's mouth: a sample delivery spout in the middle and water reward spouts to the left and right. All three spouts were connected to servo motor controllers so they can be automatically presented or retracted; licks were detected and tracked by a multi-channel capacitive touch sensor (Adafruit). The setup also housed an odor delivery tube above the sample delivery spout. The open/close states of the spouts, the delivery of the odor, and the movement of spouts were controlled by a customized MATLAB and arduino program.

To motivate licking, mice were water deprived for 24 hr. Animals had an average of 2 sessions/day of training. In a typical session, animals were trained to taste a randomly presented sweet or bitter stimulus from the sample delivery spout (~1 μl of 5mM AceK or 1mM Quinine), hold the memory of the taste during a variable delay period, and then upon presentation of an odor cue (see below), report the identity of the tastant by licking the left or right spouts for a water reward (Figure 1A). The sample delivery spout was retracted during the delay period. Mice were trained with four or three taste-odor combinations (see Figure 1A, compare 'Four-Arms' vs 'Three Arms' insets). When a bitter stimulus was followed by odor A (5% n-amyl acetate in mineral oil) at the end of the delay period, mice had to lick the right spout for a water reward. If a sweet stimulus were followed by the same odor A, animals had to lick the left spout. When a sweet stimulus was followed instead by odor B (5% benzaldehyde in mineral oil), the mice had to lick the right spout. In addition to these three taste-odor combinations, in the Four-Arm paradigm, mice were presented with the bitter-odor B combination, where animals had to lick the left spout for a water reward (Figure 1A, see 'Four-Arms' diagram). Correct responses were rewarded with ~7 μl of water; incorrect responses were not rewarded. If the first lick was to the incorrect port, the response was computed as incorrect even if the mouse then attempted to go to the opposite port for water. Below is a detailed description of the training regime:

Stage 1(1–2 days), animals were acclimated to the setup, cubicle and running wheel. Stage 2 (1–2 days), animals learned that water will be delivered from the sample delivery spout. Stage 3 (1 day), animals learned that different tastants (other than water) are delivered from the sample delivery spout. During this session, the servo controller moved the spout in front of the animal's mouth and the mouse was allowed to drink randomly presented AceK (5mM), quinine (0.25 mM for the first session and 1 mM on the second session) or water for 5 s; this was repeated for ~ 50 trials/session, with intertrial intervals of 5s. Stage 4 (1–2 days), animals learned that water can be delivered from the left and right reward spouts. Mice were allowed free drinking from either spout (performed with the sample delivery spout retracted such that only left and right spouts were available); if a strong bias was detected, only the unpreferred side spout was presented until they made ~100 licks, and then retested with both spouts. This procedure was repeated until there was no apparent bias for one spout over the other. Stage 5 (1–2 days), animals learned to drink water from the left or right spout only within the odor stimulus time window (2 s). In essence, Odor A or Odor B were randomly delivered every 10s and animals received water reward only if they licked the left or right spout during odor stimulus. Again, if a strong bias was detected, only one spout was presented. Stage 6 (1–2 days; only sweet), animals were trained with randomized sweet-odor A and sweet-odor B trials, until they made more than 75% correct choices under both conditions. The delay period in this and subsequent stages of training was 1 s. Stage 7 (3–7 days), the animals were trained with a series of micro-sessions, consisting of ten randomized sweet-odor A or sweet-odor B trials followed by five consecutive bitter-odor A trials, until the animals made more than 75% correct choices under all 3 conditions. The purpose of micro-session training was to help animals differentiate sweet and bitter stimuli. Stage 8 (7–14 days; final stage of

three-arm training before testing), the animals were trained with randomized bitter-odor A, sweet-odor A or sweet-odor B trials, until they made ~90% correct choices under all 3 conditions (with 1 s delay). Note that ~15% of the animals did not improve beyond 70% correct choices even after 14 days of stage 8 training, and were excluded from further training or testing.

For the four-arms training, mice were trained (Stages 1-8) until they made 75% correct choices (rather than 90% as in the three-arm paradigm), and then began training with all four taste-odor combinations. Stage 9 (7-10 days), mice were trained with nine randomized trials (consisting of the familiar three arms) followed by 3 consecutive bitter-odor B trials, until they attained ~70% correct choices in each of the familiar three arms (i.e. this stage ensures that introduction of the new condition does not diminish performance on the original 3 arms). Stage 10 (3-4 weeks), the animals were trained with consecutive trial blocks (four sweet-odor A trials, four bitter-odor A trials, four sweet-odor B trials, and four bitter-odor A trials), until the animals made more than 70% correct choices under all conditions. Stage 11 (2-3 weeks), the block size was reduced to 3 consecutive trials, until the animals made more than 70% correct choices under all conditions. Stage 12 (2-3 weeks), the block size was reduced to 2 consecutive trials, until the animals made more than 70% correct choices under all conditions. Stage 13 (2-3 weeks), the block size was reduced to 1 trial, until the animals made more than 75% correct choices under all conditions. Stage 14 (4-8 weeks, the final stage before testing), the animals were trained with randomized trials of the four taste-odor combinations, until the animals made more than 75% correct choices under all conditions. At this stage, the overall performance often dropped to less than 65%, so to help mice reach the learning criterion, they were iteratively trained from stage 12 to stage 14 several times. After 20 weeks of four-arms training, 30% mice showed less than 60% correct choices, and were excluded from further training or testing.

To train animals to hold a taste memory for 6 s (Figure 5C), we initially trained the animals with 1s delay until the animals made ~90% correct choices under all 3 conditions (see above), and tested with 6 s delay (1-2 sessions). Then, we continued training these animals using only a 6s delay (2-3 sessions/day), until they made more than 80% correct choices. Around 30% mice showed less than 70% correct responses after 10 days training, and were excluded from further training or testing.

To analyze facial movements during the memory task, we recorded facial images (frame rate = 20 Hz), and analyzed the videos using DeeplabCut.[60] We selected 13 features: 3 nose, 3 mouth, 4 locations on the whisker pad, and 3 eye (see Figure S7). The average feature positions during the 1s period prior to sampling the tastant were used as the baseline. Movements were quantified as trajectories from baseline for each of the 13 features for the 6.5 s duration of each trial.

Laser-stimulation in behaving mice

To activate rNST SST neurons and record evoked GCaMP6 signals in GCbt (Figure 4B), we used a blue laser (5-10 mW, 40 Hz, 5 ms pulses, 0.5 s duration), and the inter-stimulation periods were 20-40 s.

To silence rNST SST neurons (Figure 4D) during sampling, the blue laser was turned on ~0.2 s before sampling, and turned off after sampling. For silencing during the delay period (Figures 4E and S8D), the laser stimulation was carried out during the entire delay period (0.5-1.5 mW, constant stimulation, 1-3 s duration).

To silence GCbt (Figure 6B) during sampling, the blue laser was turned on ~0.2 s before sampling, and turned off after sampling. For silencing during the delay period, the laser stimulation was carried out during the entire delay period (1-3 s, Figure 6A), or last 1/3 delay period (1-2 s, Figure S10). The laser intensity was 10-15 mW, 20 Hz, 5 ms pulses.

To activate VIP neurons in GCbt during sampling (Figures S12A and S12B) or SST neurons in rNST during sampling (Figures S12C and S12D), the blue laser stimulation (10 -15 mW, 40 Hz, 5 ms pulses, 0.5 s duration) was triggered by the first sampling lick on the sample delivery spout.

To activate VIP neurons in GCbt during the delay (Figure 6C), the blue laser stimulation (10-15 mW, 40 Hz, 5 ms pulses) was applied during the initial 5 s of the delay window.

Fiber photometry

We used fiber photometry to record GCbt responses to tastants. Animals were head restrained on a running wheel. The spout was connected to a servo motor and presented in front of their mouths. The stimulus time windows were controlled by the movement of the spout. To measure the non-tastant dependent responses (e.g. water, licking) in GCbt, mice were trained to dry-lick or drink water for 0.5 s (~5 μl). To separate taste-evoked responses from non-taste responses, animals had to drink water for 8 s (~20 μl) or dry lick for 2.5 s (~15 licks) prior to tastant delivery (~1 μl of bitter or sweet stimuli). Stimuli: acesulfame K (AceK, 5 or 20 mM, Sigma-Aldrich, 04054); Quinine monohydrochloride dihydrate (Quinine, 1 or 4 mM, Sigma-Aldrich, 145920); Cycloheximide (Cyx, 0.05 mM, Sigma-Aldrich, 01810). Viral targeting and the placement of fiber implants were verified at the termination of the experiments by histology. Around 30% animals with misplaced fibers or injection sites were removed from the analysis (see Figures 2 and 3); these animals often exhibited no responses or no differences to the separate taste stimuli.

We also used fiber photometry to estimate the half decay time of spontaneous GCaMP6s activity in our in vivo recordings (see Figure S6A). Animals were placed on a running wheel and after ~5 min of acclimatization, we recorded 2 min of spontaneous activity in GCbt. Individual events were detected by a custom MATLAB program using the following thresholds for peak selection, width at half maximum > 0.2s and peak distance between events >0.4s. The half decay time (~0.37 s) is far smaller than the decay kinetics of the memory trace (2.0-2.5 s; Figures 3, 4, and 5). Similar GCaMP6s decay times have been observed in a number of other in vivo studies.[36,43–45]

Brain slice electrophysiology

Adult mice were anesthetized with ketamine/xylazine (100/10 mg/kg, intraperitoneally). Brains were dissected and placed in ice-cold oxygenated 110 mM choline chloride, 2.5 mM KCl, 0.5mM $CaCl_2$, 7mM $MgCl_2$, 1.3mM NaH_2PO_4, 25mM $NaHCO_3$, 10mM glucose, 1.3mM Na-ascorbate, 0.6mM Na-pyruvate, and 15mM sucrose. Brain coronal sections (250 μm) containing GCbt were incubated for 1 h at 34°C in oxygenated ACSF containing 125mM NaCl, 2.5mM KCl, 2mM $CaCl_2$, 1.3mM $MgCl_2$, 1.3mM NaH_2PO_4, 1.3mM Na-ascorbate, 0.6mM Na-pyruvate, 10mM glucose, and 25mM $NaHCO_3$.

For patch clamp recordings slices were superfused with ACSF (3 ml/min) at room temperature. The internal solution of the recording pipettes (3.5-4.5 MΩ) contained 140mM K-gluconate, 10mM HEPES, 0.2mM EGTA, 3mM KCl, 2mM Na_2ATP, 2mM $MgCl_2$ (pH 7.2–7.4). Voltage- and current-clamp recordings were performed with a computer-controlled amplifier (Axon 200B, Molecular Devices; USA), were low-pass filtered at 2 kHz and digitized at 10 kHz (DigiData 1440, Molecular Devices). Optogenetic-stimulation was delivered using an X-Cite Multi-Triggering LED Illumination System (XLED1).

When using VGAT-ires-Cre::Ai32 mice, GCbt neurons were recorded in the current-clamp mode; inward currents (~50 pA) were injected to evoke action potentials. VGAT-expressing neurons were optogenetically activated using a 1 s or 3 s blue light stimuli (460 nm, 20 Hz, 5 ms pulse, 3.5 mW/mm^2).

When using VIP-ires-Cre slices, neurons were recorded in the voltage-clamp mode. To examine the dis-inhibition effect of VIP neuron activation, the GCbt neurons were clamped at -50 mV. GCbt VIP expressing neurons were targeted with AAV-DIO-ChR2. Thalamo-cortical projections to GCbt (VPMpc) were targeted with AAV-CaMKII- ChrimsonR. The coordinates for injection were AP -2.1mm, ML 0.75mm, DV 4.3mm. Orange light (590 nm, 2 ms single pulse, 0.1 mW/mm^2) was used to activate the thalamo-cortical terminals in GCbt (see text for details). VIP neurons expressing ChR2 were stimulated with blue light (460 nm, 40 Hz, 2 ms pulse, 2 s, 0.2 mW/mm^2). The blue light was turned on 1 s before the orange light to ensure activation of VIP neurons prior to stimulation of the taste pathway. Orange light with or without blue light trials were interspersed with 30s in between trials.

QUANTIFICATION AND STATISTICAL ANALYSIS

Data quantification and statistical analysis was carried out using GraphPad Prism or custom MATLAB programs. Statistical tests were performed using unpaired t test, paired t test, Mann-Whitney test or Kruskal-Wallis test when appropriate. Each statistical test used was indicated in the respective figure legends. $p < 0.05$ was considered to be statistically significant.